DALTON
FULL PAPER

Effects of metal co-ordination geometry on self-assembly: a dinuclear double helicate complex and a tetranuclear cage complex of a new bis-bidentate bridging ligand

Rowena L. Paul, Samantha M. Couchman, John C. Jeffery, Jon A. McCleverty,* Zoe R. Reeves and Michael D. Ward *

School of Chemistry, University of Bristol, Cantock's Close, Bristol, UK BS8 1TS. E-mail: mike.ward@bristol.ac.uk

Received 9th December 1999, Accepted 3rd February 2000

Reaction of 3-(2-pyridyl)pyrazole with 3,3′-bis(bromomethyl)biphenyl resulted in the new ligand L^1 which contains two bidentate chelating pyrazolyl/pyridine fragments separated by a *meta*-biphenyl spacer; this ligand is designed to act only as a bridging ligand, as the two bidentate sites are too far apart to co-ordinate to the same metal ion. The dinuclear copper(II) complex $[Cu_2(L^1)_2(OAc)_2][BF_4]_2$ is a double helicate in which each copper(II) centre is in a square pyramidal co-ordination geometry, arising from two bidentate pyrazolyl/pyridine groups (one from each ligand L^1) and a monodentate acetate. The structure is stabilised by extensive inter-ligand π-stacking interactions. The complex $[Ag_2(L^1)_2][ClO_4]_2$ is also assumed to be a double helicate. In contrast, reaction with Co^{II} afforded the tetranuclear cage complex $[Co_4(L^1)_6][BF_4]_8$, in which each bridging ligand links two metal centres by spanning one edge of the Co_4 tetrahedron. Each metal is therefore in a pseudo-octahedral tris-chelate geometry, with the three bidentate chelating arms each coming from a different ligand L^1. Again there is substantial inter-ligand π stacking. Unlike other complexes with the same $\{M_4L_6\}$ tetrahedral cage structure, the central cavity is not occupied by a counter ion, showing that although the templating effect of a counter ion can be beneficial in the assembly of such cages it is clearly not essential. ^{1}H NMR spectroscopy suggests that there is a mixture of species in solution arising from other metal : ligand combinations; ^{11}B NMR spectroscopy shows that at −40 °C a $[BF_4]^-$ anion can become trapped in the cavity of the cage, giving a characteristic high-field resonance in addition to that for the free $[BF_4]^-$ anions. Reaction of L^1 with Pd^{II} afforded a mixture of products arising from ligand decomposition, of which $[Pd_2(L^1)(pypz)_2][BF_4][OH]$ was structurally characterised. It has a near-planar $\{Pd_2(\mu\text{-}pypz)_2\}^{2+}$ core [Hpypz = 3-(2-pyridyl)pyrazole, which has arisen from decomposition of L^1] with an additional bridging ligand L^1 co-ordinating in a 'basket-handle' mode, straddling the central core.

The course of a self-assembly reaction between a labile metal ion and a multidentate bridging ligand depends principally on the stereoelectronic properties of the metal ion, and the number and disposition of the binding sites of the bridging ligands.[1,2] In some cases the interaction between these is well understood and a considerable degree of control can be exerted over the self-assembly process by judicious choice of components, such that the number, denticity and disposition of the binding sites in the ligand, and the co-ordination number and geometric preferences of the metal ions, can precisely be matched to achieve a remarkable degree of specificity in the self-assembly process.[3] This is exemplified by the recent work of Raymond and co-workers who have developed a symmetry-based argument to rationalise and predict the assemblies of some quite complicated cage structures.[4]

Sometimes, however, factors other than the nature of the metal ion and the ligand need to be taken into account, a particularly significant one being incorporation of a third component, the counter ion, into the structure. Recently there have been several reports of reactions between particular metal/ligand combinations where the assembly can proceed along two different paths, depending on whether or not the counter ion exerts a templating effect.[5–8] Many of these have involved the reaction of octahedral metal ions with bis-bidentate (four-co-ordinate) bridging ligands. Such a combination is likely to lead to a metal : ligand ratio of 2 : 3 in the absence of any other strongly co-ordinating species, but more complicated structures based on cyclic double helicates and tetrahedral cages can occur in which an anion is trapped in the central cavity having fulfilled the role of a template during the assembly process.[5–8]

In one such example we recently investigated the co-ordination behaviour of the bridging ligand L^2, with two bidentate pyrazolylpyridine chelates linked by a xylylene spacer.[7] We isolated both an open-chain dinuclear complex $[Ni_2(L^2)_3]^{4+}$, and a tetranuclear tetrahedral cage $[Co_4(L^2)_6(BF_4)]^{7+}$ in which a $[BF_4]^-$ anion is trapped in the central cavity. In both cases there is the necessary 2 : 3 ratio of six-co-ordinate metal to tetradentate ligand, but in the latter case the templating effect of the $[BF_4]^-$ anion entirely changes the course of the assembly process. Reaction with Cu^I, which requires a pseudo-tetrahedral geometry, predictably afforded the dinuclear double helicate $[Cu_2(L^2)_2]^{2+}$.[9] These three examples neatly illustrate the importance of both the nature of the metal ion and the presence (or absence) of a counter ion templating effect on the course of the self-assembly.

We describe here the synthesis and co-ordination chemistry of the new ligand L^1, an analogue of L^2 but with a more extended spacer group incorporating two phenyl units instead of one. In principle all of the structural types seen for the complexes of L^2 should still be possible, but a tetrahedral $\{M_4(L^1)_6\}$ cage will have a much larger cavity, so that relatively small anions such as $[BF_4]^-$ will not be so effective as templates. We were interested to see if the assembly of complexes of L^1 proceeded along different lines because of this limitation, and the results are presented in this paper.

Results and discussion

Synthesis and crystal structure of the ligand L^1

The ligand L^1 was prepared in 65% yield by reaction of 3,3′-

DOI: 10.1039/a909702c

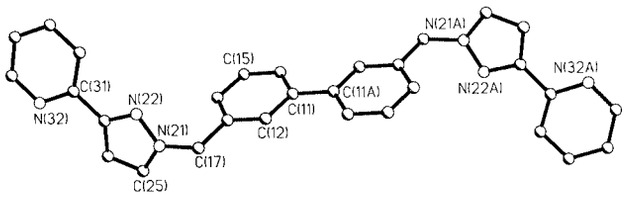

Fig. 1 Crystal structure of L^1.

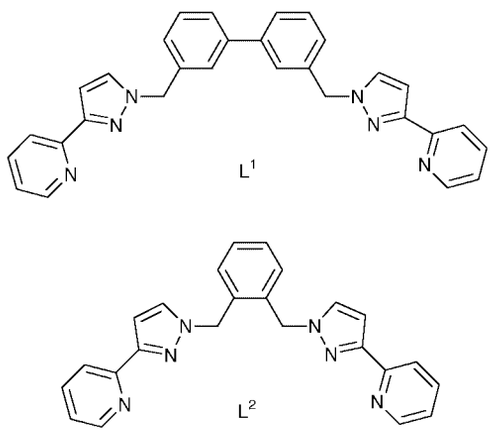

bis(bromomethyl)biphenyl with 3-(2-pyridyl)pyrazole and base under phase-transfer conditions, and satisfactorily characterised by mass and ^{1}H NMR spectroscopic data (see Experimental section). This is the same method used to prepare L^2 from 1,2-bis(bromomethyl)benzene,[7,9] and is a potentially powerful general method for the preparation of bis-bidentate bridging ligands with a wide variety of spacers.

X-Ray quality crystals were grown by diffusion of ether vapour into a concentrated solution of L^1 in CH_2Cl_2; the crystal structure is in Fig. 1. The molecule lies across an inversion centre which is located at the midpoint of the C(11)–C(11A) bond, such that the two halves are crystallographically equivalent. The pyridyl/pyrazolyl units adopt a *transoid* configuration to minimise unfavourable electronic interactions between the lone pairs of N(22) and N(32); the inter-ring torsion angle is 16°. The two rings of the central biphenyl unit in contrast are strictly coplanar. Bond distances and angles within the molecule are unremarkable. It is clear from this structure that, in contrast to the shorter ligand L^2 which contains just one phenyl spacer, it will be impossible for both bidentate arms of L^1 to co-ordinate to the same metal ion, as happened on occasion with L^2.[7,9] The new ligand L^1 can therefore only act as a bridging ligand.

Double helical complexes with Cu^{II} and Ag^I

Reaction of L^1 with copper(II) acetate hydrate in MeOH (1:1 ratio) afforded a clear green solution from which a light green solid precipitated on addition of aqueous $NaBF_4$. Electrospray mass spectrometric data indicated a 2:2 metal:ligand ratio, with the peak at highest *m/z* being 1168.7 which corresponds to $\{Cu_2(L^1)_2(BF_4)_2(H_2O)\}^+$. X-Ray quality crystals were grown by slow evaporation of a solution of the complex in MeOH, and the subsequent crystal structure determination (Fig. 2) showed the complex to be the dimer $[Cu_2(L^1)_2(OAc)_2][BF_4]_2$ (see also Table 1).

The complex is a fairly conventional double helicate, with both bridging ligands spanning both metal ions. The two copper(II) centres, which are crystallographically equivalent as the complex lies across a C_2 axis, are in a basically square pyramidal five-co-ordinate geometry arising from two bidentate pyridyl/pyrazolyl chelates and a monodentate acetate ligand. The axial ligand N(221) is more remote from the metal centre [Cu(1)–N(221), 2.247(4) Å] than are the four equatorial ligands

Table 1 Selected bond distances (Å) and angles (degrees) for $[Cu_2(L^1)_2(OAc)_2][BF_4]_2$

Cu(1)–O(2)	1.934(4)	Cu(1)–N(221)	2.247(4)
Cu(1)–N(111)	2.033(4)	Cu(1)–N(211)	2.056(4)
Cu(1)–N(121)	2.042(3)		
O(2)–Cu(1)–N(111)	169.57(14)	O(2)–Cu(1)–N(121)	94.42(14)
N(111)–Cu(1)–N(121)	80.47(14)	O(2)–Cu(1)–N(211)	90.5(2)
N(111)–Cu(1)–N(211)	93.7(2)	N(121)–Cu(1)–N(211)	172.2(2)
O(2)–Cu(1)–N(221)	97.1(2)	N(111)–Cu(1)–N(221)	93.20(14)
N(121)–Cu(1)–N(221)	108.37(14)	N(211)–Cu(1)–N(221)	76.99(14)

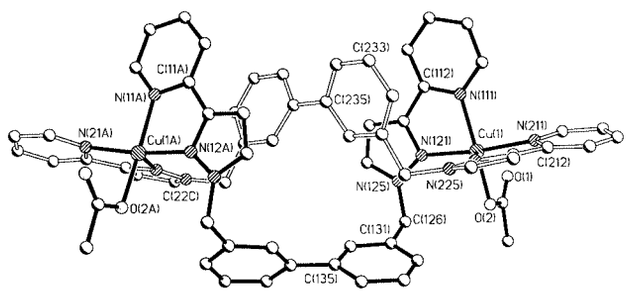

Fig. 2 Crystal structure of the complex cation of $[Cu_2(L^1)_2(OAc)_2][BF_4]_2$. One ligand strand is shown with hollow bonds for clarity.

[average 2.02 Å] in keeping with the requirements of the Jahn–Teller effect. The two bridging ligands adopt significantly different conformations. In ligand 2 [denoted by the first digit of the numbering scheme, *i.e.* N(211) and so on, depicted with hollow bonds in Fig. 2] the central biphenyl unit is involved with π-stacking interactions with both pyridyl/pyrazolyl co-ordinating units of ligand 1 (inter-planar separations in the region of 3.5 Å) to give a 'three-layer' stack. In contrast the central biphenyl unit of ligand 1 is more remote from the central core of the complex and is not involved in any intermolecular stacking interactions. This is reflected in the torsion angles between the rings within each biphenyl unit, which are 28.2° in ligand 2 (involved in π stacking) and 58.0° in ligand 1 (not involved in π stacking).

The fact that L^1 supports a double helical architecture suggests that double helicates should also form using Cu^I and Ag^I, which tend to adopt a pseudo-tetrahedral bis-chelate geometry with this sort of ligand; for example, $[Cu_2(L^2)_2]^{2+}$ is a double helicate.[9] Attempts to isolate a copper(I) complex of L^1 were unsuccessful, giving only green copper(II) complexes after work-up which are presumably similar to $[Cu_2(L^1)_2(OAc)_2]^{2+}$. We therefore prepared the complex with Ag^I, which has the same structural preference for pseudo-tetrahedral geometry as Cu^I but which is not redox-active. Reaction of L^1 with $AgClO_4$ in thf afforded a white precipitate of a material analysing as $[Ag(L^1)][ClO_4]$. Its dimeric nature was confirmed by its electrospray mass spectrum, which showed a strong peak at *m/z* 1251 corresponding to $\{Ag_2(L^1)_2(ClO_4)\}^+$. We could not isolate X-ray quality crystals despite several attempts, but the 2:2 metal:ligand stoichiometry suggests that, like the copper(II) complex, the silver(I) complex is a double helicate.

The tetranuclear cage $[Co_4(L^1)_6][BF_4]_8$

We were next interested to see what type of complex would form with a metal ion having a preference for regular octahedral geometry. In the absence of any other ligands we expect a metal:ligand ratio of 2:3, which can be achieved in several different ways. Triple helicates are well known in which all three bis-bidentate ligands bridge both metals.[10] An alternative structure with the same stoichiometry is exemplified by $[Ni_2(L^2)_3]^{4+}$,[7] in which two ligands are terminal and only one is bridging, *i.e.* $[(L^2)Ni(\mu\text{-}L^2)Ni(L^2)]^{4+}$; however this is unlikely with L^1 which cannot co-ordinate all donor sites to one metal ion because of

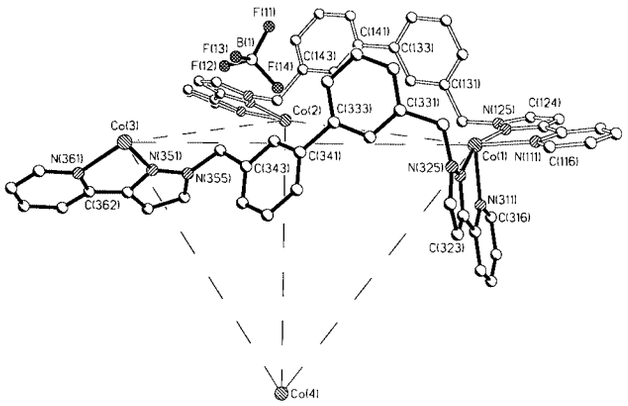

Fig. 3 Crystal structure of part of the complex cation of $[Co_4(L^1)_6][BF_4]_8 \cdot 6MeCN$, showing (i) the tetrahedral arrangement of metal ions, (ii) two of the six ligands which bridge the edges of the tetrahedron, and (iii) one of the $[BF_4]^-$ anions which is involved in weak CH · · · F hydrogen bonding interactions with the periphery of the complex cation.

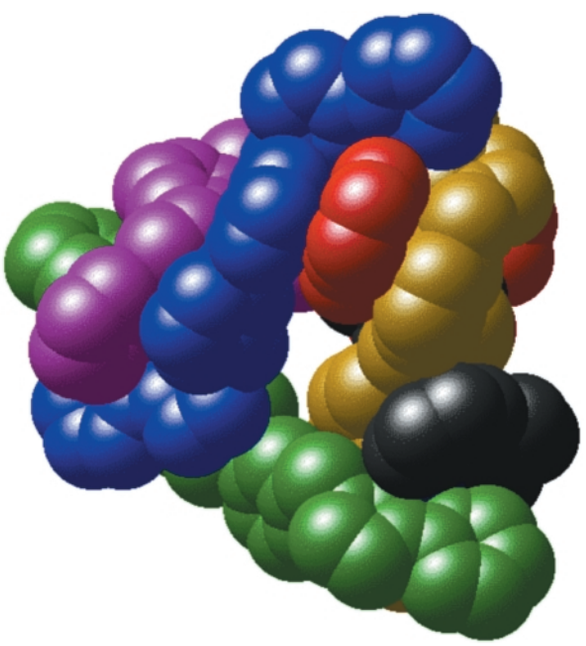

Fig. 4 Space-filling picture of the complex cation $[Co_4(L^1)_6]^{8+}$ with each ligand coloured differently, emphasising the inter-ligand π-stacking interactions and easy access to the central cavity.

the large, relatively rigid spacer between them. A cyclic helicate with a metal : ligand ratio of 8 : 12 has been observed.[9] A fourth possibility is a tetrahedral cage having six bridging ligands, one along each edge of the tetrahedron,[4,6,7] as exemplified by $[Co_4(L^2)_6(BF_4)][BF_4]_7$.[7] In this case the formation of the cage appeared to be templated by inclusion of a $[BF_4]^-$ anion in the central cavity which was an ideal fit; the larger cavity which would necessarily occur in a cage structure based on L^1 may diminish the templating action of the anion if the 'good fit' criterion is important.

Reaction of L^1 with cobalt(II) acetate hydrate in a 3 : 2 molar ratio afforded a salmon-pink solution from which a pale orange solid precipitated on addition of aqueous $NaBF_4$. The electrospray mass spectrum shows numerous peaks, with the highest *m*/*z* value of 1784.3 corresponding to $\{Co_2(L^1)_3(BF_4)_3\}^+$, indicating formation of at least a dinuclear complex. Diffusion of ether vapour into a concentrated MeCN solution of the complex afforded X-ray quality crystals; the structure of the compound is in Figs. 3 and 4.

The complex has the formulation $[Co_4(L^1)_6][BF_4]_8 \cdot 6MeCN$ (although the number of solvents quoted is an approximation due to extensive disorder, see Experimental section), and is an approximately tetrahedral cage with one bridging ligand spanning each of the six edges of the tetrahedron. Each metal ion is co-ordinated by a bidentate pyridyl/pyrazolyl unit from each of three different ligands, and has a distorted pseudo-octahedral geometry with the Co–N separations in the range 1.96–2.22 Å, characteristic of high-spin Co^{II}. Each metal centre is therefore chiral with all four metal ions having the same chirality within each tetranuclear unit. There are equal numbers of opposite enantiomers in the unit cell related by an inversion centre. This structure is topologically equivalent to those of other $\{M_4L_6\}$ tetrahedral cages based on bis-bidentate bridging ligands.[4,6,7] The structure is stabilised by multiple aromatic π-stacking interactions between overlapping adjacent ligand fragments, which are emphasised in the space-filling view of the complex in Fig. 4. The Co · · · Co separations vary between 11.49 and 12.27 Å, with the average being 11.88 Å; this is significantly larger than in $[Co_4(L^2)_6(BF_4)][BF_4]_7$ where the Co · · · Co separations are in the range 8.98–10.07 Å.[7]

The important difference between our earlier complex $[Co_4(L^2)_6(BF_4)][BF_4]_7$ and this new example $[Co_4(L^1)_6][BF_4]_8$ is that in the latter there is no $[BF_4]^-$ anion trapped in the central cavity; all of the anions are 'free' in the lattice, although there are close associations between some of the counter ions and the periphery of the metal complex. This is illustrated in Fig. 3, which depicts the Co_4 tetrahedron with only two of the six bridging ligands shown for clarity. One $[BF_4]^-$ anion is perched above the triangular face described by Co(1), Co(2) and Co(3), in a shallow pocket between the three bridging ligands associated with that face. The result is several CH · · · F contacts in which the H · · · F separations are around 2.5 Å and the C · · · F contacts are around 3.2 Å, indicative of weak CH · · · F hydrogen bonding which is well known when $[BF_4]^-$ anions are used.[11]

It is therefore apparent that the assembly of the $[Co_4(L^1)_6]^{8+}$ cage is not dictated by an anion-based template effect. This is in marked contrast to the behaviour of $[Co_4(L^2)_6(BF_4)]^{7+}$ where (i) the cage was *only* found with an encapsulated anion, which remained trapped in the central cavity on the NMR timescale; and (ii) in the absence of a templating effect, an alternative open-chain structure $[Ni_2(L^2)_3]^{4+}$ was observed. The fact that a $[BF_4]^-$ anion is not observed in the cavity of $[Co_4(L^1)_6]^{8+}$ may be ascribed partly to the large cavity size, which would make the anion a much poorer fit and reduce the favourable electrostatic interaction with the surrounding 8+ charge, and partly to the gap in the centre of each triangular face of the complex which could allow small guest molecules to drift in and out of the cavity in solution. In addition, the fact that L^1 cannot act as a tetradentate chelate to one metal ion (unlike L^2) prevents the alternative open-chain structure from forming in which there is one bridging and two terminal ligands, *cf.* $[Ni_2(L^2)_3]^{4+}$. The complex $[Co_4(L^1)_6][BF_4]_8$ is unusual amongst the few examples of this type.[4,6,7] in that (i) it has a large central cavity, and (ii) the cavity is empty; it does not even contain solvent molecules.[4] Although the template effect is clearly operative in formation of other $\{M_4L_6\}$ tetrahedra,[6,7] it does not appear to be all-important.

In the area of self-assembly using labile metals ions there is always the possibility of a mixture of species in solution even if only one form is isolated in the crystalline state. Accordingly, we examined the NMR behaviour of this complex in solution to see to what extent the solution and the solid state structures are comparable. The ^1H NMR spectrum of $[Co_4(L^1)_6][BF_4]_8$ in CD_3CN showed at least 42 resonances between δ −40 and +100. Although the ^1H NMR spectra of high-spin cobalt(II) complexes are paramagnetically shifted, it is nonetheless possible to obtain useful information from them regarding the number of magnetically inequivalent proton environments.[12] If $[Co_4(L^1)_6][BF_4]_8$ were to adopt a regular tetrahedral geometry in solution on the NMR timescale, we would expect only 12 magnetically inequivalent proton environments. Conversely, if

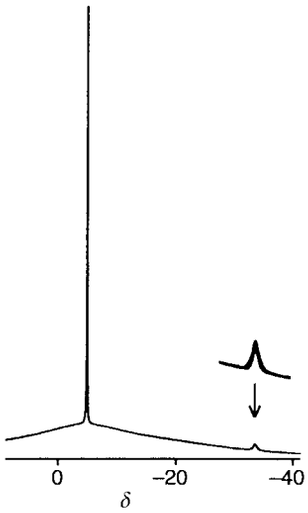

Fig. 5 ^{11}B NMR spectrum of $[Co_4(L^1)_6][BF_4]_8$ at −40 °C in CD_3CN showing the additional resonance corresponding to $[BF_4]^-$ trapped within the cavity of the tetrahedral cage.

it retained in solution a low-symmetry structure like that observed in the solid state then anything up to 144 magnetically inequivalent proton environments would occur. Therefore we have either a mixture of complexes in solution, or the one cage complex adopting a low-symmetry conformation. The appearance of this spectrum did not vary significantly with temperature.

Further insight into the solution behaviour was provided by ^{11}B NMR spectroscopy. For $[Co_4(L^2)_6(BF_4)][BF_4]_7$ the ^{11}B and ^{19}F resonances of the encapsulated $[BF_4]^-$ anion were shifted substantially upfield compared to those of the free $[BF_4]^-$ anion (^{11}B, δ −1 and −105 for free and encapsulated $[BF_4]^-$; ^{19}F, δ −150 and −242 for free and encapsulated $[BF_4]^-$).[7] For $[Co_4(L^1)_6][BF_4]_8$ in contrast, at room temperature in CD_3CN a single ^{11}B resonance is seen at δ −5. On cooling the sample an additional small signal appears at higher field which by −40 °C is quite sharp and clear at δ −34 ppm (Fig. 5). This upfield shift is consistent with a $[BF_4]^-$ ion inside the $[Co_4(L^1)_6]^{8+}$ cavity, and the temperature dependent behaviour indicates that a dynamic process is occurring in which a $[BF_4]^-$ ion can diffuse into and out from the cavity, and that this exchange process can be frozen out. The fast exchange at room temperature is presumably facilitated by the gaps in the centre of each triangular face of the complex cation which allow access to the central cavity. This is in contrast with the behaviour of $[Co_4(L^2)_6(BF_4)]^{7+}$ for which the anion remains trapped in the cavity (on the NMR timescale) at all accessible temperatures. Integration of the two peaks in Fig. 5 gives a ratio of *ca.* 1 : 10 for encapsulated *vs.* free $[BF_4]^-$ (we used a relaxation delay of 2 seconds when the spectra were accumulated to ensure that the comparison of the integrals for the two signals was as accurate as possible). If all of the complex were present as the tetrahedral cage with no other metal–ligand combinations present, and every cavity contained an anion, then a ratio of 1 : 7 would be expected. Allowing for the inevitable uncertainty in the integral values, this suggests that most of the complex is present in solution at −40 °C as the tetrahedral cage form $[Co_4(L^1)_6]^{8+}$ with an anion trapped in the cavity, in interesting contrast to the solid-state structure.

A dinuclear complex of Pd^{II} arising from partial decomposition of L^1

Having examined the co-ordination behaviour of L^1 with metals having preferences for square pyramidal [Cu^{II}], tetrahedral [Ag^I] and octahedral [Co^{II}] geometries we were interested to use a metal ion having a strong preference for square-planar co-ordination, *viz.* Pd^{II}; it is not easy to see how this stereoelectronic preference can be reconciled with the structural limitations of this ligand.

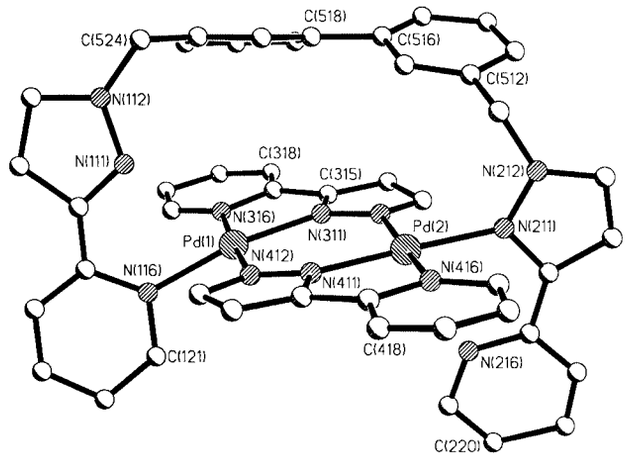

Fig. 6 Crystal structure of the complex cation of $[Pd_2(L^1)(pypz)_2][BF_4][OH]\cdot 4.5H_2O\cdot MeCN$.

Reaction of L^1 with palladium(II) acetate (1 : 1 molar ratio) in MeOH afforded an intense yellow solution, from which a yellow solid was isolated on addition of aqueous $NaBF_4$. The FAB and electrospray mass spectra of this both had their most abundant peak at *m/z* 574 with an isotope pattern characteristic of one Pd atom; this corresponds to the fragment $\{Pd(L^1)\}^+$. In addition the FAB spectrum showed a weaker peak (8% abundant) at *m/z* 680, corresponding to $\{Pd_2(L^1)\}^+$. The ^{1}H NMR spectrum of the solid showed a poorly resolved mixture of overlapping signals in the aromatic region characteristic of a mixture of products.

Recrystallisation of the crude solid by diffusion of diethyl ether vapour into a concentrated MeCN solution afforded a few crystals which were marginally suitable for an X-ray diffraction study; the result is in Fig. 6. This compound has the formulation $[Pd_2(L^1)(pypz)_2][BF_4][OH]\cdot 4.5H_2O\cdot MeCN$, and is a dinuclear palladium(II) complex in which a near-planar $\{Pd_2(\mu\text{-}pypz)_2\}^{2+}$ core is spanned by one L^1 ligand which loops over the top like a basket handle [Hpypz = 3-(2-pyridyl)-pyrazole, which has arisen from decomposition of L^1]. The palladium(II) centres both have their favoured square-planar co-ordination geometry, which is achieved by having the two potentially bidentate chelating units of L^1 acting as only monodentate ligands. Thus Pd(1) is co-ordinated to the pyridyl donor N(116) but not significantly to the associated pyrazolyl donor N(111) which adopts a pseudo-axial position with a long, weak interaction to the metal ion (2.86 Å). Similarly, Pd(2) co-ordinates the pyrazolyl donor N(211) of the other potentially chelating pocket of L^1, but the adjacent pyridyl donor N(216) only forms a very weak pseudo-axial interaction (2.89 Å). These are in obvious contrast to the four Pd–N bonds in the square plane which all lie between 1.97 and 2.07 Å. One phenyl ring from the biphenyl unit of the intact L^1 ligand [atoms C(518)–C(523)] forms a π-stacking interaction with one of the pypz ligands [atoms N(311)–C(321)] with an average interplanar separation of *ca.* 3.5 Å.

Given the poor quality of this structure (see Experimental section) there is no point in discussing the minutiae of the structural parameters in any detail; however the overall structure is clear and has some interesting features. Principally, it illustrates a clear example of a self-assembly process being dominated by the stereoelectronic requirement of the metal. Both the partial decomposition of L^1 to generate pypz units, and only monodentate co-ordination of the potentially bidentate sites of L^1, are driven by the high thermodynamic stability of Pd^{II} in a square-planar ligand field. Both of these types of behaviour have been seen before in complexes of Pd^{II} where the ligand set appeared to be poorly suited for providing a square-planar co-

ordination geometry.[13,14] It is obvious from the NMR and mass spectrometric data that this crystal structure represents but one component of a mixture of decomposition products. A FAB mass spectrum recorded on the material after recrystallisation changed dramatically from that recorded on the freshly prepared solid; the peaks at *m*/*z* 574 and 680, corresponding to $\{Pd(L^1)\}^+$ and $\{Pd_2(L^1)\}^+$ respectively, disappeared to be replaced by new peaks at *m*/*z* 915, 878, 827 and 789. Of these the peak at *m*/*z* 878 corresponds to the fragment $\{Pd_2(L^1)(pypz)\}^+$, consistent with the crystal structure, but no obvious assignments can be found for the others.

Conclusion

Reaction of the new ligand L^1 with various transition-metal ions afforded a variety of structures in which L^1 always acts as a bridging ligand. Whereas dinuclear double helicates are observed for the complexes with Cu^{II} and Ag^{I}, the complex with Co^{II} is a tetrahedral $[Co_4(L^1)_6]^{8+}$ cage with a large central cavity into which the $[BF_4]^-$ counter ions can diffuse as shown by variable-temperature ^{11}B NMR spectroscopy. Significantly, this tetrahedral $[Co_4(L^1)_6]^{8+}$ cage formed even without a strong anion-templating effect, in marked contrast to $[Co_4(L^2)_6(BF_4)]^{7+}$, although it is clearly less robust in consequence as shown by its fragmentation under mass spectrometric conditions. Reaction of L^1 with Pd^{II} resulted in decomposition of the ligand to generate pzpy ligand fragments which allowed Pd^{II} to adopt its preferred square-planar co-ordination geometry.

Experimental

General details

Instrumentation used for routine spectroscopic studies has been described previously.[2] The starting materials 3-(2-pyridyl)-pyrazole[15] and 3,3′-bis(bromomethyl)biphenyl[16] were prepared according to the literature methods.

Syntheses

L^1. A mixture of 3,3′-bis(bromomethyl)biphenyl (0.91 g, 2.68 mmol), 3-(2-pyridyl)pyrazole (0.86 g, 5.90 mmol), aqueous NaOH (10 M, 7 cm^3) and thf (50 cm^3) was heated to reflux with stirring for 24 h. After cooling the yellow solution was dried over $MgSO_4$, filtered, and the solvent removed *in vacuo* to afford an off-white solid which was shown to be impure by TLC. The crude solid was dissolved in dichloromethane and applied to a silica column using ethyl acetate–methanol (99 : 1) as eluent to yield the desired product as the third fraction. White crystals were obtained upon solvent evaporation. Yield: 0.81 g, 65%. EI mass spectrum: *m*/*z* 468 (100, M^+) and 323 (64%, M^+ − Hpypz). ^1H NMR (400 MHz, $CDCl_3$): δ 8.65 (1 H, d, *J* 4.4, pyridyl H^6), 7.97 (1 H, d, *J* 8.0, pyridyl H^3), 7.74 (1 H, pseudo-t, pyridyl H^4), 7.50–7.38 (4 H, m), 7.23–7.21 (2 H, m), 6.97 (1 H, d, *J* 2.2 Hz, pyrazolyl) and 5.44 (2 H, s, CH_2). Found: C, 76.4; H, 5.2; N, 17.6%; C_5H_4N requires C, 76.9; H, 5.2; N, 17.9%. X-Ray quality crystals were grown by slow diffusion of diethyl ether vapour into a CH_2Cl_2 solution of L^1.

$[Cu_2(L^1)_2(OAc)_2][BF_4]_2$. A solution of L^1 (0.050 g, 0.11 mmol) in CH_2Cl_2 (10 cm^3) was added dropwise to a solution of $Cu(MeCO_2)_2{\cdot}H_2O$ (0.032 g, 0.071 mmol) in MeOH (10 cm^3). After stirring the mixture at room temperature for 1 h to give a clear solution, the product was precipitated by addition of aqueous $NaBF_4$ to give a light green solid which was filtered off and dried *in vacuo*. Yield: 0.044 g, 30%. ES-MS: *m*/*z* 1168.7 (18, $\{[Cu_2L_2][BF_4]_2{\cdot}H_2O\}^+$), 1150.9 (10, $\{[Cu_2L_2][BF_4]_2\}^+$), 550.4 (65, $\{[Cu_2L_2]{\cdot}H_2O\}^{2+}$), 531.3 (100, $\{Cu_2L_2\}^{2+}$) and 265.7 (68%, $[CuL]^{2+}$). Found: C, 56.2; H, 3.5; N, 12.6%; $C_{32}H_{27}BCuF_4N_6O_2$ requires C, 56.7; H, 4.0; N, 12.4%. X-Ray quality crystals were grown by slow evaporation of a saturated methanolic solution of the complex.

$[Ag_2(L^1)_2][ClO_4]_2$. To a solution of L^1 (0.062 g, 0.12 mmol) in thf (20 cm^3) under N_2 was added solid $AgClO_4$ (0.035 g, 0.12 mmol). A white precipitate started to form immediately, and the mixture was left to stir overnight. Filtration of the solid and drying *in vacuo* afforded pure $[Ag_2(L^1)_2][ClO_4]_2$ (0.060 g, 35%). ESMS: *m*/*z* 1251 (3, $\{Ag_2(L^1)_2(ClO_4)\}^+$) and 575 (100%, $\{Ag_2L_2\}^{2+}$). Found: C, 52.9; H, 3.1; N, 12.3%; $C_{30}H_{24}AgClN_6O_4$ requires C, 53.4; H, 3.5; N, 12.5%.

$[Co_4(L^1)_6][BF_4]_8$. A solution of L^1 (0.070 g, 0.15 mmol) in CH_2Cl_2 (10 cm^3) was added dropwise to a solution of $Co(MeCO_2)_2{\cdot}4H_2O$ (0.025 g, 0.10 mmol) in MeOH (10 cm^3). The resultant salmon-pink solution was left to stir at room temperature for 1 h whereupon dropwise addition of aqueous $NaBF_4$ precipitated a pale orange solid which was filtered off and dried *in vacuo*. Yield 0.063 g, 20%. ES-MS: *m*/*z* 1784.3 (5, $\{[Co_2L_3](BF_4)_3\}^+$), 1316.2 (8, $\{Co_2L_2][BF_4]_3\}^+$), 1160.3 (34, $\{[Co_2L_2][BF_4]F\}^+$), 1014.7 (56, $\{CoL_2F\}^+$), 546.2 (100, $\{CoLF\}^+$), 527.5 (5, $\{CoL\}^+$), 469.3 (62, $\{LH\}^+$) and 263.6 (55%, $\{CoL\}^{2+}$). Found: C, 55.5; H, 3.7; N, 12.4%; $C_{180}H_{144}B_8Co_4F_{32}N_{36}{\cdot}6H_2O$ requires C, 56.1; H, 4.1; N, 13.1%. X-Ray quality crystals were grown by slow diffusion of diethyl ether vapour into a MeCN solution of $[Co_4L_6][BF_4]_8$ at 0 °C.

$[Pd_2(L^1)(pzpy)_2][BF_4][OH]$. A solution of L^1 (0.10 g, 0.22 mmol) in CH_2Cl_2 (10 cm^3) was added dropwise to a solution of $Pd(MeCO_2)_2$ (0.050 g, 0.22 mmol) in MeOH (20 cm^3). An intense yellow solution developed which was left to stir at room temperature for 1 h. An excess of aqueous $NaBF_4$ was then added dropwise and over a 10 minute period the solution became cloudy. After reducing the solvent volume by half a yellow precipitate resulted which was filtered off and dried *in vacuo*. Yield 0.18 g. FABMS: *m*/*z* 680 (8, $\{Pd_2(L^1)\}^+$), 574 (100, $\{Pd(L^1)\}^+$) and 430 (30%, $\{Pd(L^1) - pypz\}^+$). Recrystallisation of this material by diffusion of ether vapour into a concentrated MeCN solution of the complex afforded a few crystals of $[Pd_2(L^1)(pypz)_2][BF_4][OH]{\cdot}4.5H_2O{\cdot}MeCN$; the ^1H NMR spectrum of the mother liquor suggested that a mixture of many other components was present.

X-Ray crystallography

Suitable crystals were quickly transferred from the mother liquor to a stream of cold N_2 on a Siemens SMART diffractometer fitted with a CCD-type area detector. In all cases a full sphere of data was collected at low temperature using graphite-monochromatised Mo-Kα radiation. A detailed experimental description of the methods used for data collection and integration using the SMART system has been published.[17] Empirical absorption corrections were applied using SADABS,[18] and structure solution and refinement was performed with the SHELX suite of programs.[19] Table 2 contains a summary of the crystal parameters, data collection and refinement details.

Crystals of both L^1 and $[Cu_2(L^1)_2(OAc)_2][BF_4]_2$ were stable and diffracted well; these structural determinations presented no problems. In L^1 the molecule lies astride an inversion centre such that only half of it is crystallographically independent. In $[Cu_2(L^1)_2(OAc)_2][BF_4]_2$ the molecule lies astride a C_2 axis such that again only half of it is crystallographically independent.

The complex $[Co_4(L^1)_6][BF_4]_8{\cdot}6MeCN$ formed nice-looking crystals which however lost solvent very fast. After many attempts a suitable crystal was mounted without too much decomposition; nevertheless diffraction was weak and only data with $2\theta \leq 40°$ were used in the final refinement as there was no significant diffracted intensity at higher angles. Owing to the weakness of the data and the large number of parameters to refine, extensive use of geometric restraints was made to keep

Table 2 Crystallographic data for the four crystal structures

	L^1	$[Cu_2(L^1)_2(MeCO_2)_2][BF_4]_4$	$[Co_4(L^1)_6][BF_4]_8 \cdot 6MeCN$	$[Pd_2(L^1)(pypz)_2][BF_4][OH] \cdot 4.5H_2O \cdot MeCN$
Formula	$C_{30}H_{24}N_6$	$C_{64}H_{54}B_2Cu_2F_8N_{12}O_4$	$C_{192}H_{162}B_8Co_4F_{32}N_{42}$	$C_{48}H_{36}BF_4N_{13}O_{5.5}Pd_2$
M	468.55	1355.9	3987.84	1182.5
T/K	173	173	123	173
System, space group	Monoclinic, $P2_1/c$	Monoclinic, $C2/c$	Monoclinic, $P2_1/n$	Monoclinic, $C2/c$
a/Å	6.0948(8)	14.702(3)	19.221(8)	35.916(11)
b/Å	10.967(2)	20.284(4)	37.42(2)	14.059(4)
c/Å	17.606(3)	20.669(6)	31.929(9)	26.247(7)
β/°	94.07(2)	94.561(11)	90.71(2)	120.314(7)
U/Å^3	1173.9(3)	6144(3)	22963(16)	11441(6)
Z	2	4	4	8
μ/mm^{-1}	0.081	0.776	0.364	0.695
Reflections collected: total, independent, R_{int}	7270, 2679, 0.0242	19097, 6969, 0.0801	73509, 21435, 0.1179	18410, 5338, 0.1766
Final $R1$, $wR2$[a]	0.0372, 0.0968	0.0654, 0.1773	0.1576, 0.4853	0.1696, 0.4440

[a] Structure was refined on F_o^2 using all data; the value of $R1$ is given for comparison with older refinements based on F_o with a typical threshold of $F \geq 4\sigma(F)$.

the refinement stable. In particular, all aromatic rings (pyridyl, pyrazolyl and phenyl) were constrained to be regular hexagons or pentagons as appropriate; the bonded B–F distances in the $[BF_4]^-$ anions were restrained to be similar to one another, as were all of the non-bonded F · · · F distances.

Of the $[BF_4]^-$ anions, six refined well with unit site occupancy, but three more appeared which refined satisfactorily with site occupancies of 0.67 each, to give the required 8 anions. Three well behaved MeCN molecules could be identified per complex molecule; in addition, a large collection of electron-density peaks clearly corresponded to further badly disordered solvent molecules. These were all refined as carbon atoms with site occupancies of either 100 or 50% as appropriate to give a total electron density consistent with the presence of 6 MeCN molecules, although this is necessarily an approximation. There is a large apparent void in the lattice of volume *ca.* 900 Å^3 in which we could only locate a seemingly random collection of low electron-density peaks (≤1 e Å^{-3}); these could not be made to look like anything sensible and presumably arise from an extensively disordered collection of solvent molecules. Use of the 'SWAT' command during refinement to try and account for the scattering of these was not successful. The atoms of all of the solvent molecules that were located, and the atoms of the disordered $[BF_4]^-$ anions, were refined with isotropic thermal parameters. All other atoms were refined anisotropically but with isotropic restraints. Considering the problems associated with this structural determination, and the size and complexity of the problem, the final $R1$ value of 15.7% is reasonable and compares well with other refinements on similarly elaborate complexes. A table of detailed bond distances and angles is however not included.

Crystals of $[Pd_2(L^1)(pypz)_2][BF_4][OH] \cdot 4.5H_2O \cdot MeCN$ suffered from very similar problems, arising from poor crystallinity, loss of solvent and extensive disorder of solvent molecules. Again only data with $2\theta \leq 40°$ were used in the final refinement. The complex dication, one $[BF_4]^-$ anion and one MeCN molecule could be located easily but there was no obvious sign of the additional anion necessary to achieve charge balance. A group of closely spaced electron-density peaks was modelled as a cluster of hydrogen-bonded water molecules, and it is reasonable to assume that one of these could be deprotonated to give a hydroxide ion. It was necessary to apply restraints to the geometric and thermal parameters (particularly of the anion and solvent molecules) to ensure stable refinement. A table of detailed bond distances and angles is not included for this reason.

CCDC reference number 186/1843.

See http://www.rsc.org/suppdata/dt/a9/a909702c/ for crystallographic files in .cif format.

Acknowledgements

We thank the EPSRC for financial support and Dr Martin Murray for assistance with the NMR spectroscopy.

References

1 D. Philp and J. F. Stoddart, *Angew. Chem., Int. Ed. Engl.*, 1996, **35**, 1155; J.-M. Lehn, *Supramolecular Chemistry*, VCH, Weinheim, 1995; C. Piguet, G. Bernardinelli and G. Hopfgartner, *Chem. Rev.*, 1997, **97**, 2005.

2 Previous paper in this series: R. L. Paul, A. J. Amoroso, P. L. Jones, S. M. Couchman, Z. R. Reeves, L. H. Rees, J. C. Jeffery, J. A. McCleverty and M. D. Ward, *J. Chem. Soc.*, *Dalton Trans.*, 1999, 1563.

3 A. M. Garcia, D. M. Bassani, J.-M. Lehn, G. Baum and D. Fenske, *Chem. Eur. J.*, 1999, **5**, 1234; G. S. Hanan, D. Volmer, U. S. Schubert, J.-M. Lehn, G. Baum and D. Fenske, *Angew. Chem.*, *Int. Ed. Engl.*, 1997, **36**, 1842; C. Piguet, G. Hopfgartner, A. F. Williams and J.-C. G. Bünzli, *J. Chem. Soc.*, *Chem. Commun.*, 1995, 2575; C. Piguet, E. Rivera-Minten, G. Bernardinelli, J.-C. G. Bünzli and G. Hopfgartner, *J. Chem. Soc.*, *Dalton Trans.*, 1997, 421; M. Fujita, *Chem. Soc. Rev.*, 1998, **27**, 417; N. Takeda, K. Umemoto, K. Yamaguchi and M. Fujita, *Nature* (*London*), 1999, **398**, 794; B. Olenyuk, J. A. Whiteford, A. Fechtenköttner and P. J. Stang, *Nature* (*London*), 1999, **398**, 796; P. J. Stang and B. Olenyuk, *Acc. Chem. Res.*, 1997, **30**, 502.

4 T. Beissel, R. E. Powers and K. N. Raymond, *Angew. Chem.*, *Int. Ed. Engl.*, 1996, **35**, 1084.

5 B. Hasenknopf, J.-M. Lehn, G. Baum, B. O. Kneisel and D. Fenske, *Angew. Chem.*, *Int. Ed. Engl.*, 1996, **35**, 1838; R. Vilar, D. M. P. Mingos, A. J. P. White and D. J. Williams, *Angew. Chem.*, 1998, **37**, 1258.

6 D. L. Caulder, R. E. Powers, T. N. Parac and K. N. Raymond, *Angew. Chem.*, *Int. Ed.*, 1998, **37**, 1840; R. W. Saalfrank, R. Burak, A. Breit, D. Stalke, R. Herbst-Irmer, J. Daub, M. Porsch, E. Bill, M. Müther and A. X. Trautwein, *Angew. Chem.*, *Int. Ed. Engl.*, 1994, **33**, 1621; M. Scherer, D. L. Caulder, D. W. Johnson and K. N. Raymond, *Angew. Chem.*, *Int. Ed.*, 1999, **38**, 1588.

7 J. S. Fleming, K. L. V. Mann, C.-A. Carraz, E. Psillakis, J. C. Jeffery, J. A. McCleverty and M. D. Ward, *Angew. Chem.*, *Int. Ed.*, 1998, **37**, 1279.

8 P. L. Jones, K. J. Byrom, J. C. Jeffery, J. A. McCleverty and M. D. Ward, *Chem. Commun.*, 1997, 1361.

9 J. S. Fleming, K. L. V. Mann, S. M. Couchman, J. C. Jeffery, J. A. McCleverty and M. D. Ward, *J. Chem. Soc.*, *Dalton Trans.*, 1998, 2047.

10 P. Baret, D. Gaude, G. Gellon and J.-L. Pierre, *New J. Chem.*, 1997, **21**, 1255; M. Albrecht, M. Schneider and R. Frohlich, *New J. Chem.*, 1998, **22**, 753; M. Albrecht and C. Riether, *Chem. Ber.*, 1996, **129**, 829.

11 K. L. V. Mann, J. C. Jeffery, J. A. McCleverty and M. D. Ward, *J. Chem. Soc.*, *Dalton Trans.*, 1998, 3029 and references therein.

12 E. C. Constable, R. Martínez-Máñez, A. M. W. Cargill Thompson and J. V. Walker, *J. Chem. Soc.*, *Dalton Trans.*, 1994, 1585; E. C.

Constable, M. A. M. Daniels, M. G. B. Drew, D. A. Tocher, J. V. Walker and P. D. Wood, *J. Chem. Soc.*, *Dalton Trans.*, 1993, 1947.
13 M. D. Ward, J. S. Fleming, E. Psillakis, J. C. Jeffery and M. D. Ward, *Acta Crystallogr.*, *Sect. C*, 1998, **54**, 609.
14 E. C. Constable, S. M. Elder, J. Healy, M. D. Ward and D. A. Tocher, *J. Am. Chem. Soc.*, 1990, **112**, 4590.
15 A. J. Amoroso, A. M. W. Cargill Thompson, J. C. Jeffery, P. L. Jones, J. A. McCleverty and M. D. Ward, *J. Chem. Soc.*, *Chem. Commun.*, 1994, 2751; H. Brunner and T. Scheck, *Chem. Ber.*, 1992, **125**, 701.
16 M. Asakawa, P. R. Ashton, S. E. Boyd, C. L. Brown, S. Menzer, D. Pasini, J. F. Stoddart, M. S. Tolley, A. J. P. White, D. J. Williams and P. G. Wyatt, *Chem. Eur. J.*, 1997, **3**, 463.
17 P. L. Jones, A. J. Amoroso, J. C. Jeffery, J. A. McCleverty, E. Psillakis, L. H. Rees and M. D. Ward, *Inorg. Chem.*, 1997, **36**, 10; SMART and SAINT, Area-Detector Control and Integration Software, Siemens Analytical X-Ray Instruments Inc., Madison, WI, 1995.
18 SADABS, A program for absorption correction with the Siemens SMART area-detector system, G. M. Sheldrick, University of Göttingen, 1996.
19 SHELXTL 5.03 program system, Siemens Analytical X-Ray Instruments, Madison, WI, 1995.

Paper a909702c